Published in "Biochemical Pharmacology 162(): 98–108, 2019"
which should be cited to refer to this work.

PARP inhibition induces Akt-mediated cytoprotective effects through the formation of a mitochondria-targeted phospho-ATM-NEMO-Akt-mTOR signalosome

Antal Tapodi[a], Zita Bognar[a], Csaba Szabo[a,b], Ferenc Gallyas[a,c,d], Balázs Sumegi[a,c,d,*], Enikő Hocsak[a]

[a] Department of Biochemistry and Medical Chemistry, University of Pécs, Medical School, Szigeti Street 12, 7624 Pécs, Hungary
[b] Department of Medicine, University of Fribourg, Switzerland
[c] Szentágothai Research Centre, University of Pécs, Pécs, Hungary
[d] Nuclear-Mitochondrial Interactions Research Group, Hungarian Academy of Sciences, Budapest, Hungary

ARTICLE INFO

Keywords:
Oxidative stress
Poly(ADP)ribose polymerase
Mitochondrion
Akt
Signaling
Cytotoxicity

ABSTRACT

Purpose: The cytoprotective effect of poly(ADP-ribose) polymerase 1 (PARP1) inhibition is well documented in various cell types subjected to oxidative stress. Previously, we have demonstrated that PARP1 inhibition activates Akt, and showed that this response plays a critical role in the maintenance of mitochondrial integrity and in cell survival. However, it has not yet been defined how nuclear PARP1 signals to cytoplasmic Akt.

Methods: *WRL 68*, HeLa and MCF7 cells were grown in culture. Oxidative stress was induced with hydrogen peroxide. PARP was inhibited with the PARP inhibitor PJ34. ATM, mTOR- and NEMO were silenced using specific siRNAs. Cell viability assays were based on the MTT assay. PARP-ATM pulldown experiments were conducted; each protein was visualized by Western blotting. Immunoprecipitation of ATM, phospho-ATM and NEMO was performed from cytoplasmic and mitochondrial cell fractions and proteins were detected by Western blotting. In some experiments, a continually active Akt construct was introduced. Nuclear to cytoplasmic and mitochondrial translocation of phospho-Akt was visualized by confocal microscopy.

Results: Here we present evidence for a PARP1 mediated, PARylation-dependent interaction between ATM and NEMO, which is responsible for the cytoplasmic transport of phosphorylated (thus, activated) ATM kinase. In turn, the cytoplasmic p-ATM and NEMO forms complex with mTOR and Akt, yielding the phospho-ATM-NEMO-Akt-mTOR signalosome, which is responsible for the PARP-inhibition induced Akt activation. The phospho-ATM-NEMO-Akt-mTOR signalosome localizes to the mitochondria and is essential for the PARP-inhibition-mediated cytoprotective effects in oxidatively stressed cells. When the formation of the signalosome is prevented, the cytoprotective effects diminish, but cells can be rescued by constantly active Akt1, further confirming the critical role of Akt activation in cytoprotection.

Conclusions: Taken together, the data presented in the current paper are consistent with the hypothesis that PARP inhibition suppresses the PARylation of ATM, which, in turn, forms an ATM-NEMO complex, which exits the nucleus, and combines in the cytosol with mTOR and Act, resulting in Act phosphorylation (i.e. activation), which, in turn, produces the cytoprotective action via the induction of Akt-mediated survival pathways. This mechanism can be important in the protective effect of PARP inhibitor in various diseases associated with oxidative stress. Moreover, disruption of the formation or action of the phospho-ATM-NEMO-Akt-mTOR signalosome may offer potential future experimental therapeutic checkpoints.

Abbreviations: ATM, ataxia telangiectasia mutated kinase; ATP, adenosine triphosphate; EDTA, ethylenediaminetetraacetic acid; EGTA, ethylene glycol-bis(β-aminoethyl ether)-N,N,N′,N′-tetraacetic acid; FBS, fetal bovine serum; H_2O_2, hydrogen peroxide; INT, 2-(4-iodophenyl)-3-(4-nitrophenyl)-5-phenyl-2H-tetrazolium chloride; MAPK, mitogen-activated protein kinase; MEM, Eagle's minimum essential medium; mTOR, mammalian target of rapamycin protein; MTT, 3-(4,5-dimethylthiazol-2-yl)-2,5-diphenyltetrazolium bromide; NAD^+, nicotinamide adenine dinucleotide; NEMO, NF-kappa-B essential modulator; PAR, poly(ADP-ribose); PARP1, poly(ADP-ribose) polymerase 1; PIK, phosphatidylinositol 3-kinase; PBS, phosphate buffered saline; FCS, fetal calf serum; PJ34, N-(-oxo-5,6-dihydro-phenanthridin-2-yl)-N,N-dimethylacetamide HCl; PMS, N-methylphenazonium methyl sulfate; PVDF, polyvinylidene fluoride; RNS, reactive nitrogen species; ROS, reactive oxygen species; SDS, sodium dodecyl sulfate

* Corresponding author at: Department of Biochemistry and Medical Chemistry, University of Pécs, Medical School, Szigeti Street 12, 7624 Pécs, Hungary.
E-mail address: Balazs.Sumegi@aok.pte.hu (B. Sumegi).

1. Introduction

Poly(ADP-ribose)polymerase is activated by single strand DNA breaks and catalyzes the covalent coupling of branched chains of ADP-ribose (PAR) units to various nuclear proteins such as histone proteins and PARP1 itself [1,2]. Consequently, PARP1 is involved in chromatin remodeling, DNA repair, replication, transcription, and the maintenance of genomic stability [3,4]. Production of reactive oxygen species (ROS) and reactive nitrogen species (RNS) has a pivotal role in the pathogenesis of various diseases including various forms of acute and chronic inflammation and ischemia-reperfusion of the heart and brain [3,5,6]. In these diseases, DNA strand breakage, induced by ROS/RNS, leads to PARP1 over-activation. The classical pathway of PARP-mediated cell injury stipulates that PARP overactivation, and, subsequent depletion of PARP's substrate, NAD^+ and, secondarily, the cellular depletion of ATP leads to necrotic-type cell death [7–9]. Genetic deficiency, as well as pharmacological inhibition of PARP1 protects the cells from cell death induced by oxidative or nitrosative stress. PARP inhibitors have been demonstrated to exert significant cytoprotective effects and preserve or improve organ function in animal models of various pathophysiological conditions including myocardial ischemia [10], neuronal ischemia [11,12], acute lung inflammation [13], septic shock [14], multiple organ failure [15] and pancreatic damage during the pathogenesis of diabetes [16–18].

Our previous studies demonstrated that besides preserving NAD^+ and ATP levels [7], cytoprotective effect of PARP inhibition is also mediated via suppression of JNK and p38 mitogen-activated protein kinases (MAPKs) [19–21], and phosphorylation – and thereby, activation – of Akt/PKB [9,22–24]. We have previously demonstrated that PARP inhibition results in an increased expression and increased cytoplasmic localization of MAPK phosphatase-1 (MKP-1/Dusp1), and we have presented evidence that this effect is responsible for the aforementioned cytoprotective effects of PARP inhibitors [20]. In line with the importance of the Akt pathway in PARP inhibitors' cytoprotective effect, we have demonstrated that small-molecule Akt inhibitors markedly reduce the protective effect of PARP inhibitors in a model of cardiac ischemia-reperfusion [22]. However, the exact molecular processes that link the inhibition of PARP to the activation of the Akt/PKB-mediated cytosolic survival pathway have not yet been elucidated.

PARP1 is involved in DNA base-excision repair [25] and homologous recombination [26] by activating and attracting repair enzymes to DNA breaks. Ataxia telangiectasia mutated kinase (ATM) participates in homologous recombination and nonhomologous end-joining of DNA double-stranded break repair [27]. Knockout experiments on ATM and PARP1 have established that ATM knockout mice and PARP knockout mice are viable, however, ATM-PARP double mutation leads to embryonic lethality [28]. These observations have been utilized in a novel tumor therapy where ATM deficiency sensitizes the tumor cells to a PARP1 inhibitor [29], although the molecular mechanism of this synthetic lethality is not well understood. Importantly, prior studies investigating the interrelationship between the PARP and the ATM pathways have demonstrated that ATM is subject to PARP1-mediated poly(ADP-ribosyl)ation [30,31].

The aim of this study was to define the molecular mechanisms, by which the nuclear PARP1 can regulate the cytoplasmic phosphatidylinositol 3-kinase (PI3K)-Akt pathway. The results presented in the current report show that inhibition of PARP1 in oxidatively stressed cells facilitates the export of ATM from the nucleus to the cytoplasm, which, in turn, plays a role in the activation of Akt, and the subsequent cytoprotective effects, via the formation of a mitochondria-associated phospho (p)-ATM-NEMO-Akt-mTOR cytoprotective signalosome.

2. Materials and methods

2.1. Cell lines

Human *WRL 68 cells* (a HeLa derivative line that exhibits a morphology similar to hepatocytes and hepatic primary cultures]), HeLa human cervix cancer cell line, MCF7 human breast adenocarcinoma were obtained from the ATCC (Wesel, Germany). Cells were grown in Eagle's minimum essential medium (MEM) containing a 1% antibiotic-antimycotic solution and 10% fetal calf serum (FCS) in a humid 5% CO_2 atmosphere at 37 °C.

2.2. RNA interference

ATM-siRNA, mTOR-siRNA and NEMO-siRNA were purchased from Santa Cruz Biotechnology. Transfection of WRL 68, MCF7 and HeLa cells was performed with GeneJuice transfection reagent purchased from NOVAGEN according to the protocol of manufacturer. Efficacy of the RNA interference was confirmed with Western blotting using appropriate primary antibodies.

2.3. Pharmacological inhibition of PARP

The PARP inhibitor PJ34 [N-(6-oxo-5,6-dihidro-phenanthridin-2-yl)-N,N-dimethylacetamide] was purchased from Sigma, and was used at 10 μM concentration. The concentration of PJ34 was selected based on prior *in vitro* studies where the 10 μM PJ34 concentration was proven to be effective to inhibit cellular PARP activation and to produce cytoprotective effects under oxidative stress conditions [20,32].

2.4. Cell fractionation

Cells were cultured on a 10 cm dish, and treated with 0.3 mM H_2O_2 (Sigma-Aldrich) for 3 h in the presence or absence of PJ34 (10 μM0, rinsed in phosphate-buffered saline solution (PBS), pH 7.4. Afterwards, the cells were harvested in 0.5 ml ice-cold lysis buffer consisting of 20 mM Tris pH 8.0, 10 mM KCl, 2 mM Mg_2Cl, 1 mM EDTA and 1 mM EGTA and protease inhibitor cocktail (Sigma) and kept on ice for 15 min. The cells were disrupted in a Teflon–glass homogenizer. The nuclear fraction was pelleted at 750 g for 15 min and retained for further purification. The supernatant was centrifuged at 10,000*g* for 15 min, and the pellet was retained for purification of mitochondrial fraction. For cytosolic fraction, 200 μl aliquots of supernatant were completed with 6× Sample Buffer (Laemmli) and stored at -80 °C until immunoblot analysis of the cytosolic fraction. The nuclear pellet was re-suspended in 1 ml lysis buffer completed with 0.2% Triton X-100, re-homogenized, and then centrifuged at 750*g* for 15 min. The pellet was resuspended in 100 μl Laemmli sample buffer and stored at -80 °C until immunoblot analysis of the nuclear fraction. Mitochondrial pellet was washed in 1 ml Lysis buffer, then centrifuged at 10,000*g* for 15 min. Pellet was re-suspended in 100 μl Laemmli sample buffer and stored at −80 °C until immunoblot analysis of the mitochondrial fraction. Cross-contamination of the fractions were tested by immunoblotting utilizing anti-Histone H3, anti-GAPDH and anti-cytochrome oxidase (C4) primary antibodies (data not shown).

2.5. Immunoblotting

Samples were homogenized in ice-cold isotonic Tris buffer (50 mM, pH 8.0) containing 0.5 mM sodium metavanadate, 1 mM EDTA, and a protease inhibitor cocktail (1:1000; Sigma-Aldrich) as described previously.

Antigens were determined from the tissue homogenates after sonication. Proteins were precipitated by trichloroacetate, washed three times with −20 °C acetone, dissolved in Laemmli sample buffer, separated on 12% SDS-polyacrylamide gels, and transferred to nitrocellulose membranes. After the blocking phase (2 h with 3% nonfat milk in Tris-buffered saline), the membranes were probed overnight at 4 °C with antibodies recognizing the following antigens: anti-PARP1, anti-ATM, anti-p-ATM, anti-PAR, anti-NEMO, anti-C4 (were from Santa Cruz Biotechnology), anti-Histone H3, anti-GAPDH, anti-Akt, anti-p-Akt, anti-p-GSK3β, anti-mTOR, anti-His (were from Cell Signaling Technology). The membranes were washed six times for 5 min in Tris-buffered saline (pH 7.5) containing 0.2% Tween before addition of goat anti-rabbit horseradish peroxidase-conjugated secondary antibody (1:3000 dilution; Bio-Rad). The protein bands were visualized with enhanced chemiluminescence labelling using an ECL immunoblotting detection system (Amersham Biosciences). The developed films were scanned, and the pixel volumes of the bands were determined using the NIH ImageJ software, with the values in ratios of intensity. Each experiment was repeated a minimum of three times.

2.6. Cell viability assay

Viability of the WRL 68 cells was determined by colorimetric MTT assay (3-(4,5-dimethylthiazol-2-yl)-2,5-diphenyl tetrazolium bromide, Sigma-Aldrich) as described previously [20,32]. The cells were seeded onto 96 plates at a density of 10^5cells/well and cultured overnight before the experiment. After 24 h of treatment, the medium was removed and fresh MEM/FCS containing 0.5% of the water-soluble yellow dye MTT was added. The cells were then incubated for 3 h at 37 °C in an atmosphere of 5% CO_2. After 3 h the medium was removed, and the water-insoluble blue formazan dye formed stoichiometrically from MTT was solubilized by acidic isopropanol (Sigma-Aldrich). Optical densities were determined by a plate-reader (Anthos Labtech 2010) at the wavelength of 550 nm, and the values were represented as arbitrary units. All experiments were run at least in quadruplicates and repeated three times. The results are expressed as percentages of control values.

2.7. Immunoprecipitation of ATM from mitochondrial or cytoplasmic cell fractions

100 µl BioMag Goat Anti-Rabbit IgG beads (Bangs Laboratories) were washed twice with PBS in magnetic rack than magnetic beads were incubated with anti-ATM antibody (1:500 dilution in 3%BSA/PBS buffer) for 2 h at room temperature in an orbital shaker. Then beads were washed twice with PBS in a magnetic rack. Mitochondrial or cytoplasmic fractions were incubated with magnetic beads for 2 h at room temperature in an orbital shaker. Magnetic beads were washed with washing buffer 1 (20 mM Tris pH = 8.0, 150 mM NaCl, 0.5% Triton X-100), then with washing buffer 2 (20 mM Tris pH = 8.0, 150 mM NaCl). Beads were washed finally in washing buffer 3 (5 mM Tris pH = 8.0), then the precipitated ATM was eluted with 1 M ammonium-hydroxide. The eluted fraction was lyophilized than precipitated and lyophilized ATM was resolved in 100 µl 1× Laemmli sample buffer.

2.8. Cloning strategy of T308D-S473D-Akt: D_2-Akt expression plasmid

T308D-S473D double mutant recombinant Akt gene was purchased from GenCast Biotechnology. Transfection of WRL 68, MCF7 and HeLa cells were performed with GeneJuice transfection reagent purchased from NOVAGEN according to the protocol of manufacturer.

2.9. Fluorescent labeling of mitochondria with pDsRed-Mito plasmid

pDSRed-Mito plasmid was purchased from Clonetech. Transfection of WRL 68, MCF7 and HeLa cells with pDsRed-Mito plasmid was performed with GeneJuice transfection reagent purchased from NOVAGEN according to the protocol of manufacturer. The cells were imaged using Nikon Inverted Microscope Eclipse Ti-U using a 60× objective and epifluorescent illumination. The images were processed using Adobe Photoshop CS5.

2.10. Immunocytochemistry

Wild type or transfected WRL 68 cells (pDsRedMito plasmid) were seeded to poly-L-lysine-coated glass coverslips and cultured at least overnight before the experiment. After subjecting the cells to the appropriate treatment (indicated in the figure legends), the coverslips were rinsed twice in PBS and then fixed in 4% paraformaldehyde at 4 °C for 20 min. Cells were permeabilized with 0.5% Triton-X100 in PBS at room temperature for 10 min, then cells were rinsed three times in PBS. Afterwards the cells were incubated with 10% BSA in PBS for 40 min at room temperature to block unspecific binding of antibodies. WRL 68 cells were incubated with p-ATM (1:100 dilution) primary antibodies diluted in 10% BSA in PBS for 1 h at room temperature. Following three times PBS washing the cells were incubated with the anti-rabbit Alexa Fluor 488 secondary antibody (1:200 dilution, Life Technologies) in 10% BSA in PBS for 1 h at room temperature in dark. The cells were washed three times in PBS prior to mounting in Vectashield Mounting Medium with DAPI (Vector Laboratories). The cells were imaged using Nikon Inverted Microscope Eclipse Ti-U using a 60× objective and epifluorescent illumination. The images were processed using Adobe Photoshop CS5.

2.11. Statistics

All data are expressed as means ± SEM from replicate determinations. ANOVA with a post hoc correction was used to determine differences. Student's *t* test was used to compare the mean values from the two groups. Differences were regarded as significant at $p < 0.05$.

3. Results

3.1. Effect of PARP inhibition on cell survival and Akt activation in oxidative stress

Previously, we reported that PARP inhibition increased survival of WRL68 cells in oxidative stress, and activation of Akt was significantly involved in this protective effect [9]. In the present study, we reproduced these results by using PJ34, the inhibitor we used in the previous report, at different concentrations. Oxidative stress was induced by exposing the cells to 0.3 mM H_2O_2 for 3 h. Viability was measured by the MTT assay while Akt activation was assessed by immunoblotting using anti p-Ser^{473}-Akt primary antibody. In agreement with the previous results, PJ34 did not affect viability of the control cells at the concentrations tested, and markedly reduced oxidative stress induced cell death (Fig. 1A) and elevated Akt phosphorylation (Fig. 1B) at concentrations above 1 µM. We examined the effect of PARP inhibition on 1.5 mM sodium nitroprusside (SNP) induced stress besides the H_2O_2 induced one. In these experiments we tested two additional PARP inhibitors recently approved for human clinical practice of cancer therapy; olaparib and veliparib as well as PARP1 silencing by using specific siRNA technique (Fig. 2). Olaparib, veliparib and PARP1 silencing reduced both H_2O_2− (Fig. 2A) and SNP (Fig. 2B) induced cell death and enhanced Akt phosphorylation (Fig. 2) both in the presence and absence of oxidative-nitrosative stress in about the same extent as PJ34 did.

3.2. Interaction between ATM and PARP1 in oxidative stress

Since PARP1 was reported to PARylate itself as well as to PARylate ATM during oxidative stress [30,31], we hypothesized an interaction between these two proteins. To test whether an interaction between PARP1 and ATM exists in cells subjected to oxidative stress, we expressed Myc-tagged recombinant PARP1 in WRL68 cells. Cells were

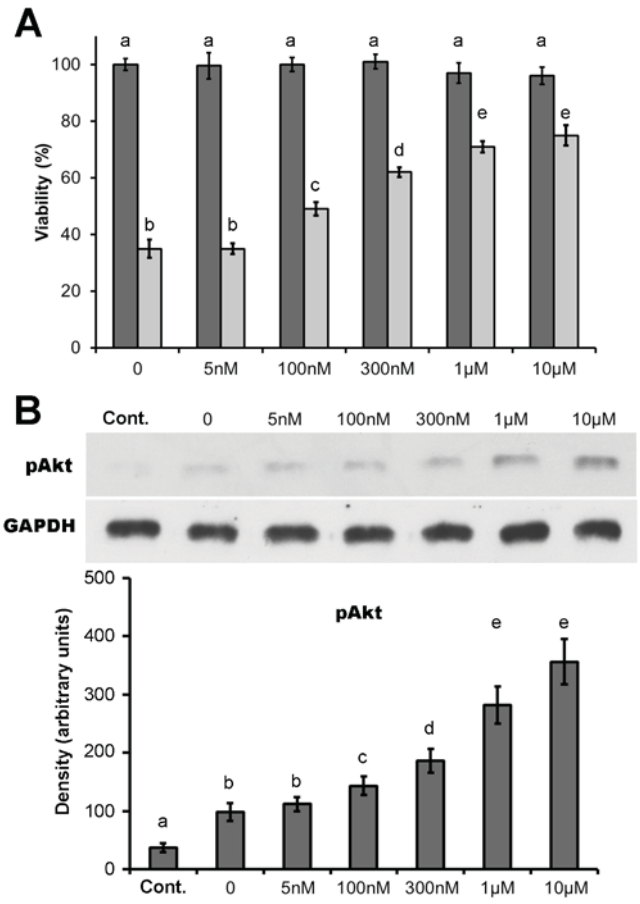

Fig. 1. Effect of PJ34 on cell survival and Akt activation in oxidative stress. WRL-68 cells were treated (light bars) or not (dark bars) with 0.3 mM H_2O_2 for 3 h in the presence or absence of different concentrations of PJ34 as indicated. Cell viabilities (A) were determined by MTT assay and expressed as % viabilities of the untreated wild type cells, means ± S.E.M. of three independent experiments. In a parallel experiment of the same treatment protocol, the cell homogenates were subjected to immunoblotting (B) utilizing anti-p-Akt primary antibody. The results are presented as representative blots as well as pixel densities of the bands, means + S.E.M. of three independent experiments. GAPDH was used as a loading control. Significantly different groups ($p < 0.05$) are indicated by lower case letters above the bars.

subjected to 0.3 mM of H_2O_2 in the presence or absence of 10 μM of PJ34. Three hours later, recombinant Myc-tagged PARP1 was pulled-down by anti-myc antibody immobilized to anti-rabbit secondary antibodies conjugated to magnetic beads. PARP1 and ATM were visualized by immunoblotting utilizing anti-PARP1 and anti-ATM primary antibodies. The experiments revealed an interaction between PARP and ATM; this interaction markedly increased in response to H_2O_2 and was diminished by PJ34 (Fig. 3A). PJ34 alone did not affect the low-level basal PARP1- ATM interaction that was detected in the absence of oxidative stress (Fig. 1A). Although, when activated, PARP1 PARylates itself as well as ATM [30,31], electrostatic repulsion between the negatively charged PAR-residues cannot explain these results, indicating that other factors must be involved in the PARP1-ATM interaction.

Next, we investigated whether PARP1 activity modulates the intracellular distribution of ATM. To this end, we treated wild type WRL68 cells as above, and visualized ATM from the cytoplasmic and the nuclear fraction of the cells by immunoblotting using an anti-ATM primary antibody. We observed that the oxidative stress decreased the cytosolic ATM levels, an effect that was diminished by PARP1 inhibition (Fig. 3B). PJ34 itself did not have any significant effect on the

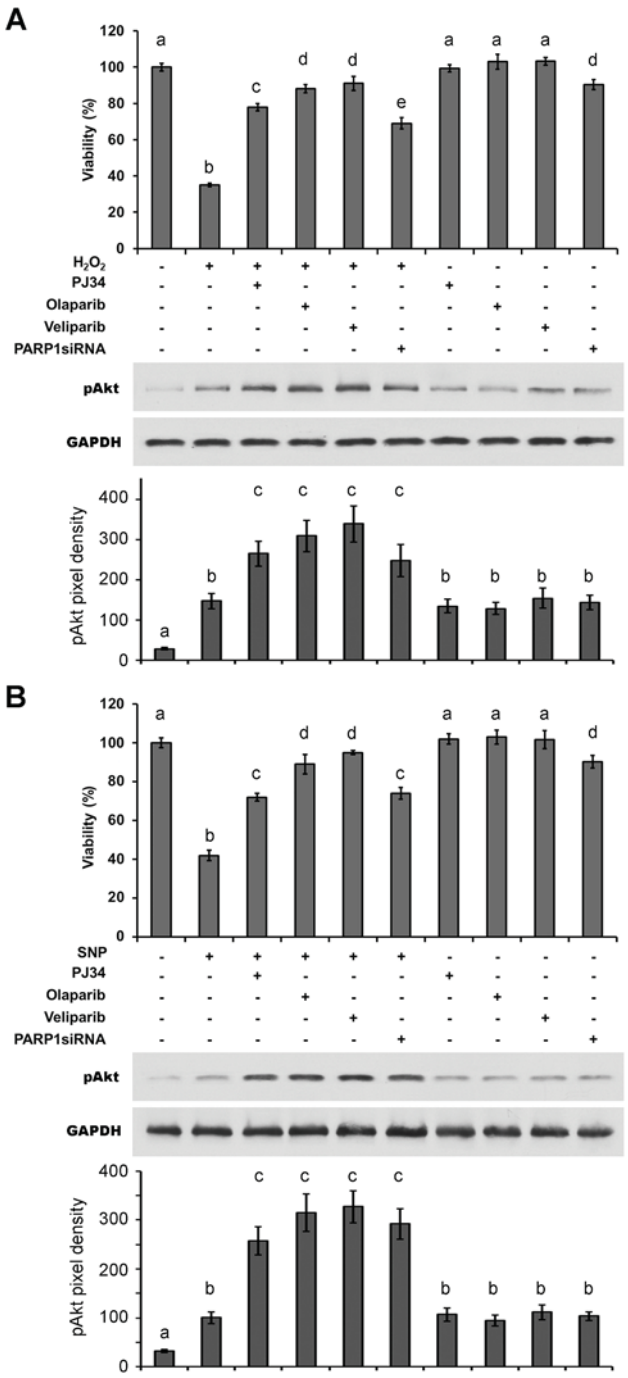

Fig. 2. Effect of PJ34, olaparib, veliparib and PARP1 silencing on cell survival and Akt activation in oxidative and nitrosative stress. WRL-68 cells were transfected with a PARP1siRNA expressing plasmid. Wild type and the transfected cells were treated with 0.3 mM H_2O_2 (A) or 1.5 mM SNP (B) for 3 h in the presence or absence of 10 μM PJ34, 100 nM olaparib or 100 nM veliparib as indicated. Cell viabilities were determined by MTT assay and expressed as % viabilities of the untreated wild type cells, means ± S.E.M. of three independent experiments. In a parallel experiment of the same treatment protocol, the cell homogenates were subjected to immunoblotting utilizing anti-p-Akt primary antibody. The results are presented as representative blots as well as pixel densities of the bands, means + S.E.M. of three independent experiments. GAPDH was used as a loading control. Significantly different groups ($p < 0.05$) are indicated by lower case letters above the bars. The treatment protocols are indicated above the representative blots, but apply to viability and pixel density bar diagrams too.

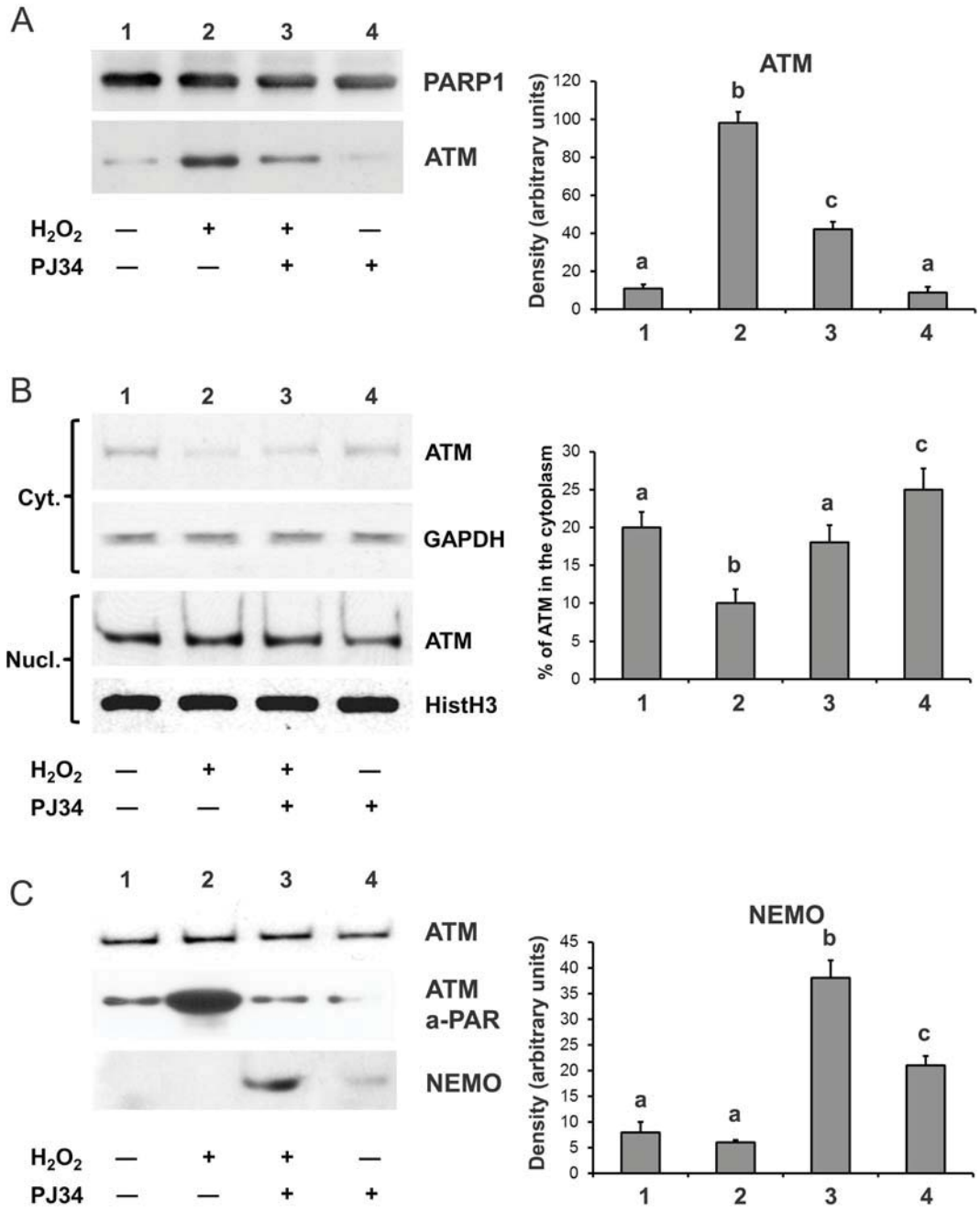

Fig. 3. Interaction of ATM, PARP1 and NEMO in WRL68 cells in oxidative stress. Myc-tagged PARP1 was overexpressed in WRL68 cells, and the cells were treated with 0.3 mM H_2O_2 for 3 h in the presence or absence of the pharmacological PARP1 inhibitor PJ34 as indicated. Recombinant Myc-tagged PARP1 was pulled-down by anti-Myc magnetic beads, then PARP1 and ATM were determined by immunoblotting (A) utilizing anti-PARP1 and anti-ATM primary antibodies from the solubilized precipitate. In a parallel experiment, wild type WRL 68 cells were subjected to the same treatment protocol. ATM levels in cytosolic and nuclear fraction of the cells (B) were determined by immunoblotting utilizing anti-ATM primary antibody. Using a separate batch of treated cells, ATM was pulled-down by anti-ATM magnetic beads, then ATM and NEMO (C) were determined by immunoblotting utilizing anti-ATM and anti-NEMO primary antibodies from the solubilized precipitate. PARylation of ATM was demonstrated by immunoblotting utilizing anti-PAR primary antibody. The results are presented as representative blots as well as pixel densities of the bands, means + S.E.M. of three independent experiments. GAPDH and PARP1 were used as loading controls, as indicated. Significantly different groups ($p < 0.05$) are indicated by lower case letters above the bars.

amount of cytoplasmic ATM detected (Fig. 3B). No significant differences in nuclear ATM were detected in the four experimental conditions utilized (Fig. 3B). These findings are consistent with the hypothesis (but does not prove) that the PARP-ATM interaction detected in Fig. 3A results in the translocation of a portion of the cellular ATM from the cytosol to the nucleus.

3.3. PARP1 inhibition results in an interaction between ATM and NEMO

Previous studies demonstrated that NEMO is responsible for the nuclear export of ATM [33]. To determine whether an interaction also exists between ATM and NEMO (and whether this interaction is modulated by oxidative stress and PARP1 activity), we employed an experimental design

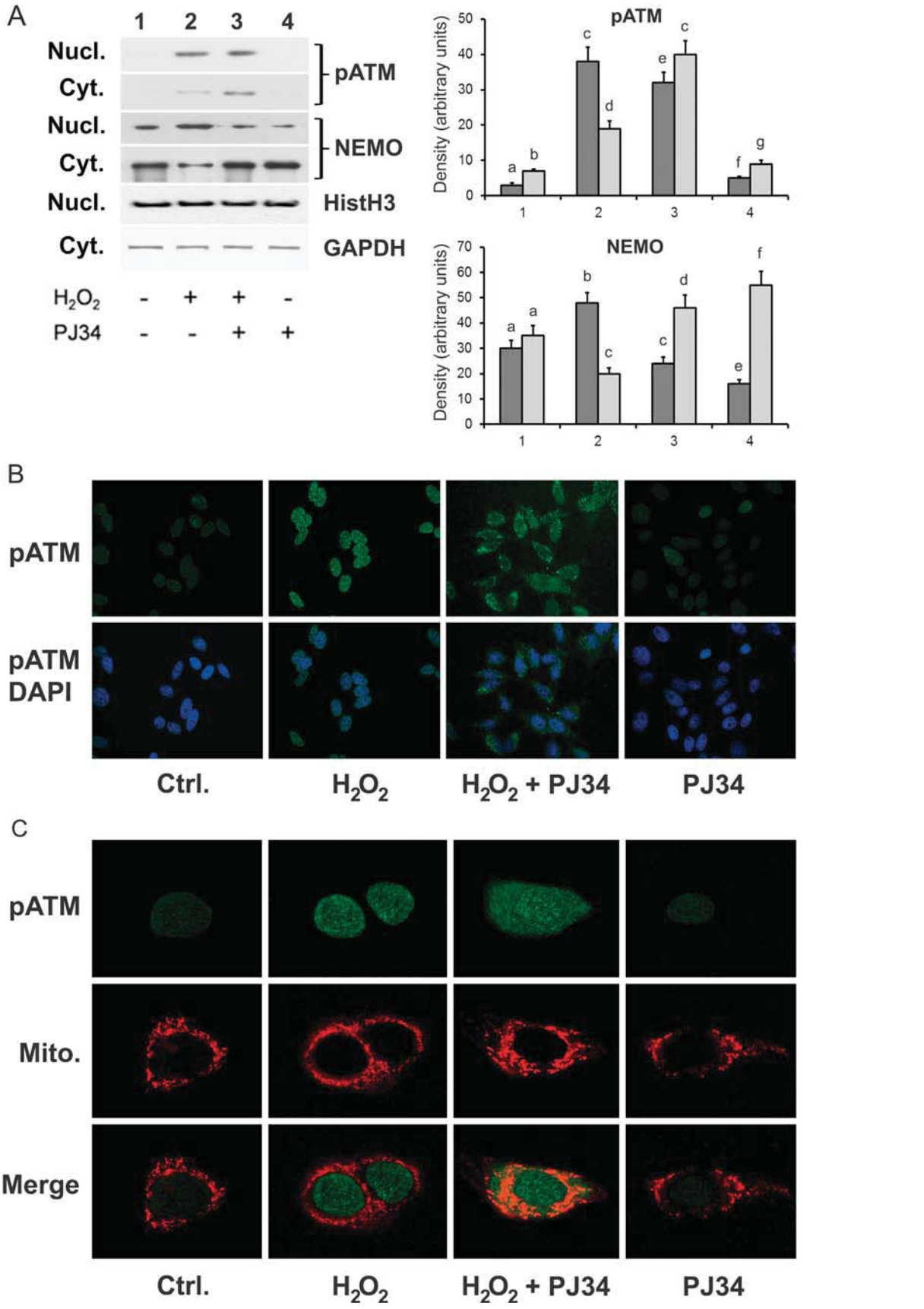

(caption on next page)

Fig. 4. Altered subcellular distribution of p-ATM and NEMO caused by PARP inhibition in oxidative stress. WRL-68 cells were treated with 0.3 mM H_2O_2 for 3 h in the presence or absence of PJ34 as indicated. Cytoplasmic (Cyt. and light bars) and nuclear (Nucl. and dark bars) fraction of the cells were subjected to immunoblotting (A) utilizing anti-phospho (p)-ATM and anti-NEMO primary antibodies. The results are presented as representative blots as well as pixel densities of the bands, means + S.E.M. of three independent experiments. GAPDH and histone H3 were used as loading controls, as indicated. Significantly different groups ($p < 0.05$) are indicated by lower case letters above the bars. The numbers above the blots indicate the treatment protocol of the groups in the bar diagram. In a parallel experiment, WRL-68 cells were treated as above. After the treatment, immunocytochemistry and confocal fluorescent microscopy were performed on the fixed and permeabilized cells utilizing anti-p-ATM primary and anti-rabbit-Alexafluor488 secondary antibodies. Nuclei were counterstained by DAPI. The results are presented as representative images (B) of three independent experiments from the green as well as the merged green and blue channels. Alternatively, mitochondria were labelled (red) by transfecting WRL-68 cells with pDsRedMito expression plasmid before the cells were exposed to the same treatment protocol. After the treatment, immunocytochemistry and confocal fluorescent microscopy were performed on the fixed and permeabilized cells utilizing anti-p-ATM primary and anti-rabbit-Alexafluor488 secondary antibodies. The results are shown as representative images (C) of three independent experiments from the green and red channels. For indicating co-localization, merged images of green and red fluorescence of the same field are also demonstrated. Mito. denotes mitochondrial staining.

similar to the one used for detecting PARP1-ATM interaction, with appropriate modifications. We pulled-down ATM by an anti-ATM antibody immobilized to anti-rabbit secondary antibodies conjugated to magnetic beads, and subsequently determined ATM and NEMO from the precipitate by immunoblotting utilizing anti-ATM and anti-NEMO primary antibodies. In contrast to the PARP1-ATM interaction, ATM-NEMO co-precipitation was close to the detection limit both under basal and oxidative stress conditions (Fig. 3C). The PARP inhibitor significantly increased the ATM-NEMO interaction in control cells (in the absence of oxidative stress); this effect was however markedly more pronounced during oxidative stress (Fig. 3C). These data are consistent with the hypothesis that PARP1 catalytic activity has a functional role in the NEMO-mediated nuclear-to-cytoplasmic export of ATM.

3.4. PARP1 inhibitor induces export of phospho (p)-ATM from the nucleus

Activation of ATM involves autophosphorylation (Ser^{1981}) and dissociation to monomers, followed by further autophosphorylation (Ser^{367}, Ser^{1893}) [34]. To determine whether the subcellular distribution of p-ATM is regulated by PARP activity in cells subjected to oxidative stress, WRL-68 cells were treated with 0.3 mM H_2O_2 for 3 h in the presence or absence of 10 μM PJ34. Subsequently, immunoblotting was performed using anti-p-ATM and anti-NEMO primary antibodies from nuclear and cytoplasmic extracts of the cells. Phosphorylation of ATM in the nuclear fraction was increased in H_2O_2 treated cells, both in the presence and absence of the PARP inhibitor (Fig. 4A: p-ATM, Nucl.). Thus, oxidative stress induces ATM phosphorylation, and this process is independent of PARP's catalytic activity. Importantly, a significant amount of phosphorylated ATM translocated to the cytoplasmic fraction in oxidatively stressed cells, *and this effect was markedly enhanced in the presence of the PARP inhibitor* (Fig. 4A: p-ATM, Cyt.). We also determined intracellular distribution of NEMO, the interacting partner of ATM [33]. Nuclear NEMO level was increased in oxidative stress while the PARP1 inhibitor diminished it both in control cells and in cells subjected to oxidative stress (Fig. 4A: NEMO, Nucl.). Cytoplasmic NEMO levels followed a pattern that was complementary to that of the nuclear fraction (Fig. 4A: NEMO, Cyt.).

Next, we sought to determine the intracellular localization of pATM translocated from the nucleus due to PARP1 inhibition during oxidative stress. To this end, WRL-68 cells were transfected with pDsRedMito expression plasmid that directs red fluorescence to the mitochondria. The transfected cells were treated with 0.3 mM H_2O_2 for 3 h in presence or absence of 10 μM PJ34, fixed, permeabilized, stained with anti-p-ATM primary and anti-rabbit Alexa Fluor 488 secondary antibodies, then analyzed by confocal microscopy. In agreement with the immunoblot results, we observed faint green fluorescence in the untreated or PJ34 treated cells. Oxidative stress induced a marked enhancement of the green fluorescence that was located to the nucleus, while the fluorescence spread to the whole cell when the cell was also co-treated with PJ34 (Fig. 4B). DAPI counterstaining (blue) helped in visualization of the cells. At higher magnification (Fig. 4C), red mitochondria located fluorescence dominated the merged images in control conditions (in the absence of oxidative stress). Oxidative stress induced the phosphorylation of ATM, as indicated by intense green

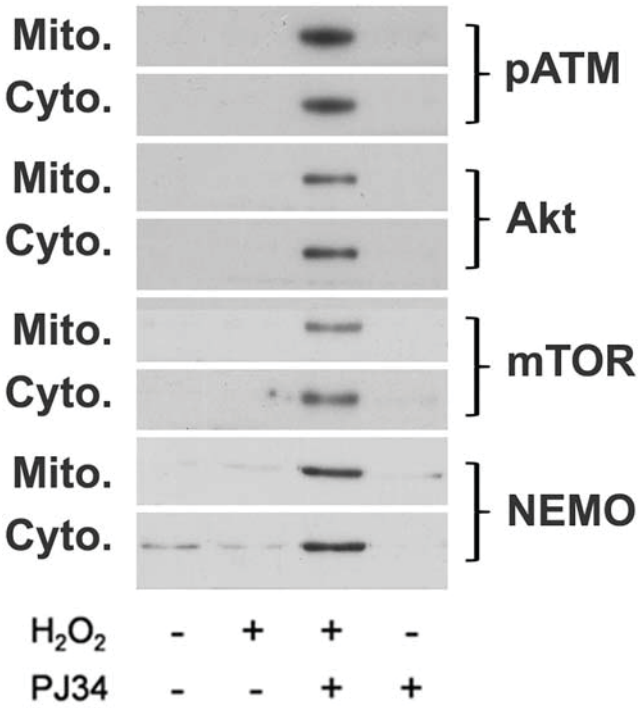

Fig. 5. Proteins co-immunoprecipitating with p-ATM from subcellular fractions of WRL-68 cells in oxidative stress and PARP1 inhibition. WRL-68 cells were treated with 0.3 mM H_2O_2 for 3 h in the presence or absence of PJ34 as indicated, then p-ATM was pulled-down by anti-p-ATM magnetic beads from cytoplasmic and mitochondrial fractions of the cells. Solubilized precipitates were subjected to immunoblotting utilizing anti-p-ATM, anti-Akt, anti-mTOR and anti-NEMO primary antibodies. The results are presented as representative blots. Mito. and Cyto. denote mitochondrial and cytosolic fractions, respectively.

fluorescence that was localized to the nucleus in the absence of PJ34, but was present in the whole cell in the presence of PJ34 (Fig. 4C). In the latter case, p-ATM appeared mostly to co-localize with the red mitochondria, as indicated by the orange color in the merged image (Fig. 4C).

3.5. Co-precipitation of Akt, mTOR and NEMO with p-ATM

The above data demonstrate that PARP1 inhibition under oxidative stress conditions activates the cytoplasmic transport of p-ATM. The data are also consistent with published data [33] showing that the cytoplasmic transport of p-ATM occurs in a NEMO-dependent manner. The above observations raise the possibility of an extra-nuclear signalosome formation. To examine whether such a signalosome, indeed, may exist, we immunoprecipitated p-ATM from cytosolic and mitochondrial fractions of WRL 68 cells treated with 0.3 mM H_2O_2 for 3 h in presence or absence of 10 μM PJ34, and detected the co-precipitated proteins by immunoblotting utilizing anti-p-ATM, anti-Akt, anti-mTOR and anti-

NEMO primary antibodies. The results show that Akt, mTOR and NEMO all co-precipitate with p-ATM in the cytosolic and mitochondrial fractions, but this interaction is only detectable in the cells that were treated by PJ34 as well as H_2O_2 (Fig. 5) supporting the existence of a signalosome comprising p-ATM, mTOR, AKT and NEMO, the formation of which is regulated by PARP catalytic activity, and which is, at least partially, associated with the mitochondria.

3.6. Silencing of the various signalosome components impairs the cytoprotective effect of PARP1 inhibition

To assess the functional significance of the above signalosome in mediating the cytoprotective effect of PARP inhibition, we systematically silenced its putative components (ATM, NEMO and mTOR) by using siRNA technique. For eliminating cell-specific effects, we used human HeLa cervix cancer and MCF7 breast carcinoma cell lines in addition to the WRL-68 line in these experiments. Efficacy of gene silencing of the target proteins was confirmed in all three cell lines by immunoblotting utilizing anti-ATM, anti-NEMO and anti-mTOR primary antibodies (Fig. 6A). The ATM-, NEMO- or mTOR silenced and wild type control cells were treated with 0.3 mM H_2O_2 for 3 h in the presence or absence of 10 μM PJ34, then viability was determined by the MTT assay. We observed significant cytoprotective effect of the PARP inhibitor in all three cell lines. However, this cytoprotective effect was abolished by ATM, NEMO, or mTOR silencing (Fig. 6B). These data indicate that cytoprotective effect of PARP inhibition in oxidatively stressed cells, is, indeed, mediated by the cytosolic translocation of the p-ATM-NEMO complex and also suggests that an interaction with mTOR is also functionally important. Taken together, the above data are consistent with a working model where, in oxidatively stress cells, the PARP-inhibition-induced activation of the cytoprotective p-AKT-mTOR cytosolic pathway is the consequence of a nuclear signal, which originates from the prevention of the PARylation of nuclear ATM, externalizes from the nucleus to the cytosol by p-ATM-NEMO and signals to downstream effector(s), at least in part via a process that also involves a mitochondrial interaction.

3.7. The role of ATM, NEMO, and mTOR in Akt phosphorylation

To determine the role of ATM, NEMO and mTOR in the activation of the Akt pathway, silenced and wild type WRL68, HeLa and MCF7 cells were treated with 0.3 mM H_2O_2 for 3 h in the presence or absence of 10 μM PJ34. The cellular proteins were subjected to immunoblotting using anti p-Ser^{473}-Akt primary antibody. In the wild type cells, we observed a faint baseline phosphorylation of Akt that was increased by either H_2O_2 or PJ34. However, when both H_2O_2 and PJ34 were present in the medium, phosphorylation thereby activation of Akt was markedly enhanced (Fig. 6C). This markedly elevated Akt phosphorylation was abolished by silencing ATM, NEMO or mTOR (Fig. 4C). These results confirm that formation of the aforementioned signalosome could account for the PARP-inhibition induced activation of the cytoprotective p-AKT-mTOR cytosolic pathway.

3.8. When the assembly of the ATM-NEMO-mTOR-Akt signalosome is prevented, a continuously active recombinant Akt (T308D-S473D-Akt: D_2Akt) restores a cytoprotective phenotype

To assess the functional importance of Akt activation due to PARP inhibition in oxidative stress, we constructed a plasmid expressing continuously active Akt (D_2Akt) that was His-tagged for enabling determination of its expression level. We transfected WRL68 cells with ATM-siRNA and/or D_2Akt expressing plasmids in different combinations. Then, we treated the cells with 0.3 mM H_2O_2 for 3 h in the presence or absence of 10 μM PJ34. Cell viability was detected by MTT assay, while whole cell extracts from a parallel experiment were subjected to immunoblotting utilizing anti-p-Akt and anti-His primary antibodies for determining phospho-Akt and D_2Akt levels, and anti-p-GSK3β primary antibody for confirming Act activation (since GSK3β is a downstream target of Akt).

Recombinant D_2Akt did not have any effect on cell survival either in baseline conditions (in the absence of oxidants) or during oxidative stress (Fig. 7A). In contrast, PJ34 protected against the oxidative stress induced loss of cell viability; this cytoprotective effect was significantly diminished by ATM silencing. However, in cells expressing D_2Akt, a cytoprotective phenotype was preserved, even when ATM was silenced (and therefore the formation of the signalosome was no longer allowed)

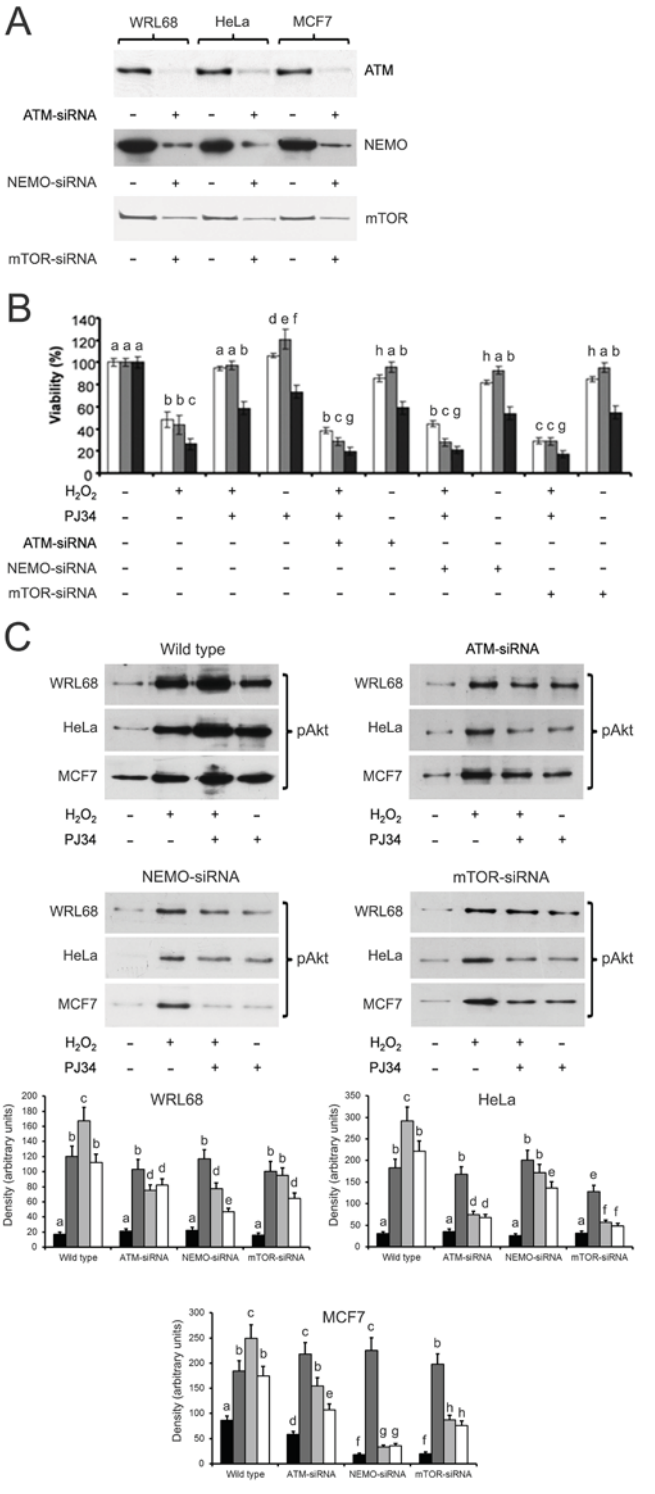

(caption on next page)

Fig. 6. Silencing of ATM, NEMO or mTOR abolishes the cytoprotective effect of PARP1 inhibition in oxidative stress. WRL68 (light bars), HeLa (grey bars) and MCF (dark bars) cells were transfected with ATM-siRNA-, NEMO-siRNA or mTOR-siRNA expressing plasmids as indicated. Wild-type and the transfected cells were treated with 0.3 mM H_2O_2 for 3 h in the presence or absence of PJ34 as indicated. Efficacy of gene-silencing (A) was checked by immunoblotting utilizing anti-ATM, anti-NEMO and anti-mTOR primary antibodies and demonstrated as representative blots of three independent experiments. Cell viabilities (B) were determined by MTT assay and expressed as % viabilities of the untreated wild type cells, means ± S.E.M. of three independent experiments. P-Akt levels of the cells (C) were determined by immunoblotting utilizing anti-p-Akt primary antibody and presented as representative blots as well as pixel densities of the bands, means + S.E.M. of three independent experiments. Untreated control, H_2O_2 only, H_2O_2 + PJ34 and PJ34 only groups are indicated as black, dark grey, light grey and white bars, respectively. Significantly different groups ($p < 0.05$) are indicated by lower case letters above the bars.

(Fig. 7A). This result suggests that activation of Akt is downstream from PARP inhibition and signalosome formation and can be viewed as a distal regulator of cell survival in oxidatively stressed cells. The observed patterns of both D_2Akt expression and GSK3β phosphorylation (indicator of Akt activation) (Fig. 7B) are fully consistent with this view. His-tagged Akt was present only in lanes 6 and 7 that was accompanied with increased phospho-Akt levels and markedly enhanced phosphorylation of GSK3β in these lanes (Fig. 7B), while faithfully reflecting Akt activation, GSK3β phosphorylation was faint in untreated baseline controls *(lane 1)*, strengthened under PARP1 inhibition in control cells (without oxidative stress) *(lane 4)* or cells subjected to oxidative stress *(lane 2)*, and was even more pronounced when PARP1 was inhibited in oxidatively stressed cells *(lane 3)*. The latter response was diminished by ATM-siRNA *(lane 5)*, while ATM-siRNA alone *(lane 8)* did not affect GSK3β phosphorylation (Fig. 7B).

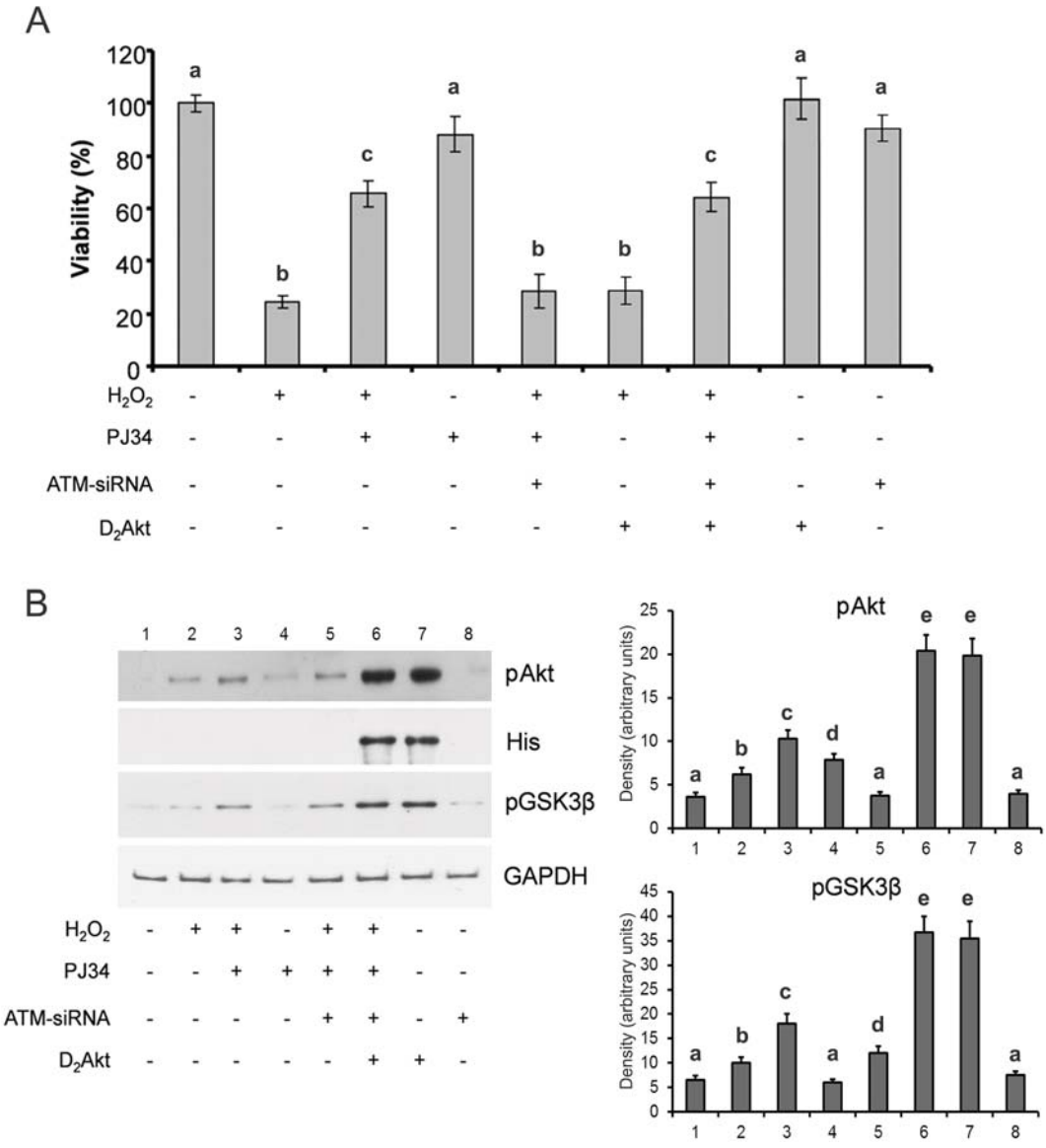

Fig. 7. Continuously active recombinant Akt (T308D-S473D-Akt: D_2Akt) counteract ATM silencing's deleterious effect on PARP inhibition induced cytoprotection. WRL-68 cells were transfected with ATM-siRNA and C-terminal-polyHis tagged D_2Akt expressing plasmids in different combinations as indicated. Wild type and the transfected cells were treated with 0.3 mM H_2O_2 for 3 h in the presence or absence of PJ34 as indicated. Cell viabilities (A) were determined by MTT assay and expressed as % viabilities of the untreated wild type cells, means ± S.E.M. of three independent experiments. In a parallel experiment of the same treatment protocol, the cell homogenates were subjected to immunoblotting (B) utilizing anti-p-Akt, anti-His and anti-p-GSK3β (downstream target of Akt) primary antibodies. The results are presented as representative blots as well as pixel densities of the bands, means + S.E.M. of three independent experiments. GAPDH was used as a loading control. Significantly different groups ($p < 0.05$) are indicated by lower case letters above the bars. The numbers above the blots indicate the treatment protocol of the groups in the bar diagram.

4. Discussion

PARP inhibitors are now clinically used for cancer therapy [33,34,35], but there is also a second line of evidence indicating their potential utility in various non-oncological diseases, many of which are associated with the overproduction of ROS and RNS, which, in turn, induces deleterious PARP overactivation; under these conditions PARP inhibitors exert cytoprotective and anti-inflammatory effects (4). In the context of cancer therapy, cytoprotective effects of PARP inhibitors may limit their efficacy as anticancer agents [35]. Namely, PARP inhibition can regulate kinase cascades such as PI3K-Akt [9,24] and MAPK [20,21] pathways, and protect mitochondrial membrane integrity [36–38]. Previously, we reported that a PARP1-ATF4-MKP1-MAPK retrograde signaling pathway is involved in the MAPK downregulating effect of PARP1 inhibition [20,32]. In the present study, we found that above the concentration of 1 μM, PJ34 diminished H_2O_2 induced death of WRL68 cells, and increased Akt activation (Fig. 1). Additionally, olaparib and veliparib, the PARP inhibitors used in human clinical practice of cancer therapy, as well as PARP1 silencing protected the cells against H_2O_2 and SNP induced stress while enhanced Akt activation in about the same extent as PJ34 did (Fig. 2). These results confirmed previous findings by us [9] and others [39–41], and underline the significance of Akt activation in PARP inhibition's protective effect in various disease models [3,22,42–44]. Therefore, in the present study we made an effort to understand the yet elusive molecular mechanism connecting PARP inhibition and Akt activation.

ATM was reported to be involved in the phosphorylation and activation of Akt in some cancer cell lines, in insulin treated myocytes, and under cellular stress conditions [45–47]. A defect in ATM-mediated Akt activation was indicated as a significant factor in the development of diabetes and neurodegenerative diseases, and ATM was suggested as a therapeutic target in cancer [47]. Additionally, PARP1 was found to PARylate ATM [30,31]. Consequently, we investigated whether a PARP1-ATM interaction is present in oxidatively stressed cells. We have utilized the WRL 68 cell line, which was used previously to demonstrate the importance of PARP1 inhibition in Akt activation [9]. Consistent with these findings, we observed that pharmacological inhibition of PARP1 stimulated the nuclear-to-cytosolic translocation of ATM, and it also enhanced a PARP1-ATM interaction both in control cells and during oxidative stress (Fig. 3A, B). Furthermore, the data presented in the current report demonstrate that inhibition of the oxidative stress-induced PARylation of ATM promotes the association of phosphorylated (and, therefore, active) ATM with NEMO (Fig. 3C). Following their cytosolic translocation, we have presented evidence for the formation of a p-ATM-NEMO-Akt-mTOR signalosome (Fig. 5). By two separate methods (Figs. 4C and 5), we demonstrated that this signalosome was, at least partially, localized to the mitochondria; an excellent position to exert mitochondria protecting effect of the PARP1 inhibition in oxidative stress. The data presented in the current report are consistent with the crucial importance of Akt activation in PARP1's cytoprotective effect: both cytoprotection and phosphorylation of Akt's downstream target, GSK3β are preserved when continuously active Akt was expressed in ATM silenced cells while ATM silencing itself abolished these effects (Fig. 7). Finally, the data are consistent with the hypothesis that the aforementioned signalosome is involved in mediating PARP1's extranuclear effects (Fig. 6), since silencing any of its components abolished Akt-activating and cytoprotective effect of the PARP1 inhibitor. Although all three human cell lines we used for these experiments are of tumor origin, the uniform results suggest that aforementioned role of the p-ATM-NEMO-Akt-mTOR signalosome may be universal.

PARP1 inhibition was reported to induce synthetic lethality in ATM suppressed or mutated cells [29], although molecular mechanism of this effect remained unclear. Apparently, inactivation of these two DNA-repair enzymes is lethal. However, in this study, we presented evidence that although suppression of ATM together with PARP inhibition caused cell death, overexpression of the active mutant T308D-S473D-Akt1 can rescue these cells (Fig. 7). These data indicate that the synthetic lethality of ATM-suppressed or ATM-mutated cells induced by PARP1 inhibitor is predominantly due to the lack of Akt1 activation. These data provide a mechanistic basis for and emphasize the significance of using PARP inhibitors in combination with PI3K-Akt inhibitors for tumor therapy. PARP1 inhibitors promote cell death by inhibiting DNA repair leading to lethal accumulation of mutations in the rapidly proliferating tumor cells. They are most effective in tumors having deleterious mutations in other DNA repair systems; therefore PARP1 inhibitors are used as a monotherapy in BRCA mutations carrying cancers [48]. However, the PARP-inhibitor-induced activation of the cytoprotective PI3K-Akt pathway in oxidatively stressed cells can cause cytostatic resistance undermining its cytostatic effect [35]. Some reports support this notion by demonstrating increased cytostatic efficacy of PARP1 inhibitors when used in combination with Akt inhibitors [35,49,50].

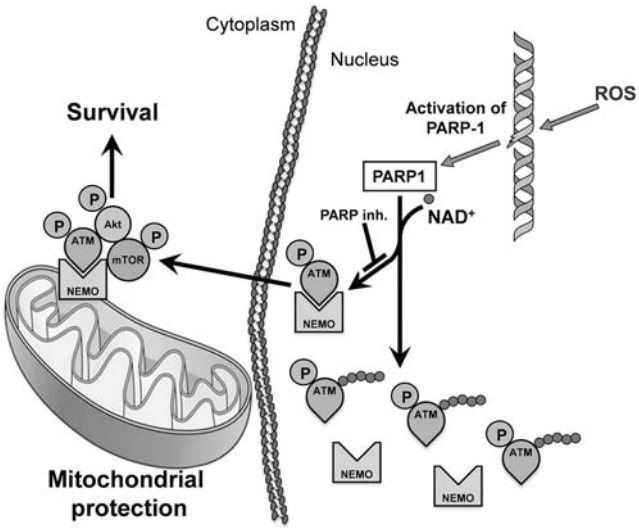

Fig. 8. A working model of the mode of PARP1 inhibition's molecular mechanism of Akt activation and cell survival in oxidatively stressed cells. PARP inhibition increases p-ATM-NEMO interaction, thereby facilitating cytoplasmic translocation of the p-ATM-NEMO complex, and the consequent formation of the p-ATM-NEMO-Akt-mTOR cytoprotective signalosome. Assembly of the signalosome leads to Akt activation, which, in turn, activates various cell survival. pathways Arrows with pointed and flat end represent activation and inhibition, respectively. P indicates phosphorylation.

In conclusion, we presented evidence for a regulatory role of PARP1 in inducing a nuclear-to-cytosolic transport of phosphorylated ATM kinase. This process initiates in the nucleus by oxidative stress induced double-stranded DNA breaks, which, in turn, induces PARP activation, and the PARylation of ATM. In parallel, oxidative stress also induces a PARP-independent phosphorylation of ATM. In turn, the results are consistent with the formation of a p-ATM-NEMO-Akt-mTOR signalosome. This signalosome is, at least partially, localized to the mitochondria, and appears to play a pivotal role in Akt activation and protection against oxidative-stress-related cell death (Fig. 8). Additionally, the data presented in the current report suggest that ATM deficiency and PARP inhibition-dependent synthetic lethality is the consequence of lacking Akt activation, providing a theoretical basis for combining Akt inhibition with PARP inhibition in the context of tumor therapy.

Acknowledgements

This work was supported by the University of Pécs, Medical School (PTE ÁOK-KA-2013/31), and by GINOP-2.3.2-15-2016-00049 and 2.3.3-15-2016-00025.

References

[1] P. Bai, Biology of poly(ADP-ribose) polymerases: the factotums of cell maintenance, Mol Cell. 58 (6) (2015) 947–958.
[2] D. D'Amours, S. Desnoyers, I. D'Silva, G.G. Poirier, Poly(ADP-ribosyl)ation reactions in the regulation of nuclear functions, Biochem. J. 342 (1999) 249–268.
[3] N.A. Berger, V.C. Besson, A.H. Boulares, A. Burkle, A. Chiarugi, R.S. Clark, N.J. Curtin, S. Cuzzocrea, T.M. Dawson, V.L. Dawson, G. Hasko, L. Liaudet, F. Moroni, P. Pacher, P. Radermacher, A.L. Salzman, S.H. Snyder, F.G. Soriano, R.P. Strosznajder, B. Sumegi, R.A. Swanson, C. Szabo, Opportunities for the repurposing of PARP inhibitors for the therapy of non-oncological diseases, Br. J. Pharmacol. 175 (2) (2018) 192–222.
[4] P.O. Hassa, S.S. Haenni, C. Buerki, N.I. Meier, W.S. Lane, H. Owen, M. Gersbach, R. Imhof, M.O. Hottiger, Acetylation of poly(ADP-ribose) polymerase-1 by p300/CREB-binding protein regulates coactivation of NF-kappaB-dependent transcription, J. Biol. Chem. 280 (49) (2005) 40450–40464.
[5] H. Kawagishi, T. Finkel, Unraveling the truth about antioxidants: ROS and disease: finding the right balance, Nat. Med. 20 (7) (2014) 711–713.
[6] M. Narasimhan, N.S. Rajasekaran, Exercise, Nrf2 and antioxidant signaling in cardiac aging, Front. Physiol. 7 (2016) 241.
[7] H.C. Ha, S.H. Snyder, Poly(ADP-ribose) polymerase is a mediator of necrotic cell death by ATP depletion, Proc. Natl. Acad. Sci. USA 96 (24) (1999) 13978–13982.
[8] P. Pacher, C. Szabo, Role of the peroxynitrite-poly(ADP-ribose) polymerase pathway in human disease, Am. J. Pathol. 173 (1) (2008) 2–13.
[9] A. Tapodi, B. Debreceni, K. Hanto, Z. Bognar, I. Wittmann, F. Gallyas Jr., G. Varbiro, B. Sumegi, Pivotal role of Akt activation in mitochondrial protection and cell survival by poly(ADP-ribose)polymerase-1 inhibition in oxidative stress, J. Biol. Chem. 280 (42) (2005) 35767–35775.
[10] B. Zingarelli, A.L. Salzman, C. Szabo, Genetic disruption of poly (ADP-ribose) synthetase inhibits the expression of P-selectin and intercellular adhesion molecule-1 in myocardial ischemia/reperfusion injury, Circ Res. 83 (1) (1998) 85–94.
[11] M.J. Eliasson, K. Sampei, A.S. Mandir, P.D. Hurn, R.J. Traystman, J. Bao, A. Pieper, Z.Q. Wang, T.M. Dawson, S.H. Snyder, V.L. Dawson, Poly(ADP-ribose) polymerase gene disruption renders mice resistant to cerebral ischemia, Nat. Med. 3 (10) (1997) 1089–1095.
[12] M. Endres, Z.Q. Wang, S. Namura, C. Waeber, M.A. Moskowitz, Ischemic brain injury is mediated by the activation of poly(ADP-ribose)polymerase, J. Cereb. Blood. Flow. Metab. 17 (11) (1997) 1143–1151.
[13] L. Liaudet, P. Pacher, J.G. Mabley, L. Virag, F.G. Soriano, G. Hasko, C. Szabo, Activation of poly(ADP-Ribose) polymerase-1 is a central mechanism of lipopolysaccharide-induced acute lung inflammation, Am. J. Respir. Crit. Care Med. 165 (3) (2002) 372–377.
[14] F.G. Soriano, L. Liaudet, E. Szabo, L. Virag, J.G. Mabley, P. Pacher, C. Szabo, Resistance to acute septic peritonitis in poly(ADP-ribose) polymerase-1-deficient mice, Shock 17 (4) (2002) 286–292.
[15] C. Szabo, L.H. Lim, S. Cuzzocrea, S.J. Getting, B. Zingarelli, R.J. Flower, A.L. Salzman, M. Perretti, Inhibition of poly (ADP-ribose) synthetase attenuates neutrophil recruitment and exerts antiinflammatory effects, J. Exp. Med. 186 (7) (1997) 1041–1049.
[16] V. Burkart, Z.Q. Wang, J. Radons, B. Heller, Z. Herceg, L. Stingl, E.F. Wagner, H. Kolb, Mice lacking the poly(ADP-ribose) polymerase gene are resistant to pancreatic beta-cell destruction and diabetes development induced by streptozocin, Nat. Med. 5 (3) (1999) 314–319.
[17] M. Masutani, H. Suzuki, N. Kamada, M. Watanabe, O. Ueda, T. Nozaki, K. Jishage, T. Watanabe, T. Sugimoto, H. Nakagama, T. Ochiya, T. Sugimura, Poly(ADP-ribose) polymerase gene disruption conferred mice resistant to streptozotocin-induced diabetes, Proc. Natl. Acad. Sci. USA 96 (5) (1999) 2301–2304.
[18] A.A. Pieper, D.J. Brat, D.K. Krug, C.C. Watkins, A. Gupta, S. Blackshaw, A. Verma, Z.Q. Wang, S.H. Snyder, Poly(ADP-ribose) polymerase-deficient mice are protected from streptozotocin-induced diabetes, Proc. Natl. Acad. Sci. USA 96 (6) (1999) 3059–3064.
[19] L. Mester, A. Szabo, T. Atlasz, K. Szabadfi, D. Reglodi, P. Kiss, B. Racz, A. Tamas, F. Gallyas Jr., B. Sumegi, E. Hocsak, R. Gabriel, K. Kovacs, Protection against chronic hypoperfusion-induced retinal neurodegeneration by PARP inhibition via activation of PI-3-kinase Akt pathway and suppression of JNK and p38 MAP kinases, Neurotox. Res. 16 (1) (2009) 68–76.
[20] B. Racz, K. Hanto, A. Tapodi, I. Solti, N. Kalman, P. Jakus, K. Kovacs, B. Debreceni, F. Gallyas Jr., B. Sumegi, Regulation of MKP-1 expression and MAPK activation by PARP-1 in oxidative stress: a new mechanism for the cytoplasmic effect of PARP-1 activation, Free Radic. Biol. Med. 49 (12) (2010) 1978–1988.
[21] B. Veres, B. Radnai, F. Gallyas Jr., G. Varbiro, Z. Berente, E. Osz, B. Sumegi, Regulation of kinase cascades and transcription factors by a poly(ADP-ribose) polymerase-1 inhibitor, 4-hydroxyquinazoline, in lipopolysaccharide-induced inflammation in mice, J. Pharmacol. Exp. Ther. 310 (1) (2004) 247–255.
[22] K. Kovacs, A. Toth, P. Deres, T. Kalai, K. Hideg, F. Gallyas Jr., B. Sumegi, Critical role of PI3-kinase/Akt activation in the PARP inhibitor induced heart function recovery during ischemia-reperfusion, Biochem. Pharmacol. 71 (4) (2006) 441–452.
[23] A. Palfi, A. Toth, G. Kulcsar, K. Hanto, P. Deres, E. Bartha, R. Halmosi, E. Szabados, L. Czopf, T. Kalai, K. Hideg, B. Sumegi, K. Toth, The role of Akt and mitogen-activated protein kinase systems in the protective effect of poly(ADP-ribose) polymerase inhibition in Langendorff perfused and in isoproterenol-damaged rat hearts, J. Pharmacol. Exp. Ther. 315 (1) (2005) 273–282.
[24] B. Veres, F. Gallyas Jr., G. Varbiro, Z. Berente, E. Osz, G. Szekeres, C. Szabo, B. Sumegi, Decrease of the inflammatory response and induction of the Akt/protein kinase B pathway by poly-(ADP-ribose) polymerase 1 inhibitor in endotoxin-induced septic shock, Biochem. Pharmacol. 65 (8) (2003) 1373–1382.
[25] M. Javle, N.J. Curtin, The role of PARP in DNA repair and its therapeutic exploitation, Br. J. Cancer 105 (8) (2011) 1114–1122.
[26] S. Xie, O. Mortusewicz, H.T. Ma, P. Herr, R.Y. Poon, T. Helleday, C. Qian, Timeless interacts with PARP-1 to promote homologous recombination repair, Mol. Cell 60 (1) (2015) 163–176.
[27] M.A. Serrano, Z. Li, M. Dangeti, P.R. Musich, S. Patrick, M. Roginskaya, B. Cartwright, Y. Zou, DNA-PK, ATM and ATR collaboratively regulate p53-RPA interaction to facilitate homologous recombination DNA repair, Oncogene 32 (19) (2013) 2452–2462.
[28] J. Menisser-de Murcia, M. Mark, O. Wendling, A. Wynshaw-Boris, G. de Murcia, Early, embryonic lethality in PARP-1 Atm double-mutant mice suggests a functional synergy in cell proliferation during development, Mol. Cell Biol 21 (5) (2001) 1828–1832.
[29] C.T. Williamson, H. Muzik, A.G. Turhan, A. Zamo, M.J. O'Connor, D.G. Bebb, S.P. Lees-Miller, ATM deficiency sensitizes mantle cell lymphoma cells to poly(ADP-ribose) polymerase-1 inhibitors, Mol. Cancer Ther. 9 (2) (2010) 347–357.
[30] R. Aguilar-Quesada, J.A. Munoz-Gamez, D. Martin-Oliva, A. Peralta, M.T. Valenzuela, R. Matinez-Romero, R. Quiles-Perez, J. Menissier-de Murcia, G. de Murcia, M. Ruiz de Almodovar, F.J. Oliver, Interaction between ATM and PARP-1 in response to DNA damage and sensitization of ATM deficient cells through PARP inhibition, BMC Mol. Biol. 8 (2007) 29.
[31] S.S. Lee, C. Bohrson, A.M. Pike, S.J. Wheelan, C.W. Greider, ATM kinase is required for telomere elongation in mouse and human cells, Cell Rep. 13 (8) (2015) 1623–1632.
[32] E. Hocsak, V. Szabo, N. Kalman, C. Antus, A. Cseh, K. Sumegi, K. Eros, Z. Hegedus, F. Gallyas Jr., B. Sumegi, B. Racz, PARP inhibition protects mitochondria and reduces ROS production via PARP-1-ATF4-MKP-1-MAPK retrograde pathway, Free Radic. Biol. Med. 108 (2017) 770–784.
[33] Z.H. Wu, Y. Shi, R.S. Tibbetts, S. Miyamoto, Molecular linkage between the kinase ATM and NF-kappaB signaling in response to genotoxic stimuli, Science 311 (5764) (2006) 1141–1146.
[34] C.J. Bakkenist, M.B. Kastan, DNA damage activates ATM through intermolecular autophosphorylation and dimer dissociation, Nature 421 (6922) (2003) 499–506.
[35] A. Szanto, E.E. Hellebrand, Z. Bognar, Z. Tucsek, A. Szabo, F. Gallyas Jr., B. Sumegi, G. Varbiro, PARP-1 inhibition-induced activation of PI-3-kinase-Akt pathway promotes resistance to taxol, Biochem. Pharmacol. 77 (8) (2009) 1348–1357.
[36] I. Racz, K. Tory, F. Gallyas Jr., Z. Berente, E. Osz, L. Jaszlits, S. Bernath, B. Sumegi, G. Rabloczky, P. Literati-Nagy, BGP-15 – a novel poly(ADP-ribose) polymerase inhibitor – protects against nephrotoxicity of cisplatin without compromising its antitumor activity, Biochem. Pharmacol. 63 (6) (2002) 1099–1111.
[37] L. Virag, C. Szabo, Purines inhibit poly(ADP-ribose) polymerase activation and modulate oxidant-induced cell death, FASEB J. 15 (1) (2001) 99–107.
[38] S.W. Yu, H. Wang, M.F. Poitras, C. Coombs, W.J. Bowers, H.J. Federoff, G.G. Poirier, T.M. Dawson, V.L. Dawson, Mediation of poly(ADP-ribose) polymerase-1-dependent cell death by apoptosis-inducing factor, Science 297 (5579) (2002) 259–263.
[39] K. Erdelyi, P. Pacher, L. Virag, C. Szabo, Role of poly(ADP-ribosyl)ation in a 'two-hit' model of hypoxia and oxidative stress in human A549 epithelial cells in vitro, Int. J. Mol. Med. 32 (2) (2013) 339–346.
[40] K. Li, Y. Li, J. Mi, L. Mao, X. Han, J. Zhao, Resveratrol protects against sodium nitroprusside induced nucleus pulposus cell apoptosis by scavenging ROS, Int. J. Mol. Med. 41 (5) (2018) 2485–2492.
[41] T. Radovits, L.N. Lin, J. Zotkina, D. Gero, C. Szabo, M. Karck, G. Szabo, Poly(ADP-ribose) polymerase inhibition improves endothelial dysfunction induced by reactive oxidant hydrogen peroxide in vitro, Eur. J. Pharmacol. 564 (1–3) (2007) 158–166.
[42] C.J. Lord, A. Ashworth, PARP inhibitors: synthetic lethality in the clinic, Science 355 (6330) (2017) 1152–1158.
[43] K. Magyar, L. Deres, K. Eros, K. Bruszt, L. Seress, J. Hamar, K. Hideg, A. Balogh, F. Gallyas Jr., B. Sumegi, K. Toth, R. Halmosi, A quinazoline-derivative compound with PARP inhibitory effect suppresses hypertension-induced vascular alterations in spontaneously hypertensive rats, Biochim. Biophys. Acta 1842 (7) (2014) 935–944.
[44] S. Veto, P. Acs, J. Bauer, H. Lassmann, Z. Berente, G. Setalo Jr., G. Borgulya, B. Sumegi, S. Komoly, F. Gallyas Jr., Z. Illes, Inhibiting poly(ADP-ribose) polymerase: a potential therapy against oligodendrocyte death, Brain 133 (Pt 3) (2010) 822–834.
[45] M.J. Halaby, J.C. Hibma, J. He, D.Q. Yang, ATM protein kinase mediates full activation of Akt and regulates glucose transporter 4 translocation by insulin in muscle cells, Cell Signal. 20 (8) (2008) 1555–1563.
[46] V. Stagni, I. Manni, V. Oropallo, M. Mottolese, A. Di Benedetto, G. Piaggio, R. Falcioni, D. Giaccari, S. Di Carlo, F. Sperati, M.T. Cencioni, D. Barila, ATM kinase sustains HER2 tumorigenicity in breast cancer, Nat. Commun. 6 (2015) 6886.
[47] D.Q. Yang, M.J. Halaby, Y. Li, J.C. Hibma, P. Burn, Cytoplasmic ATM protein kinase: an emerging therapeutic target for diabetes, cancer and neuronal degeneration, Drug Discov. Today 16 (7–8) (2011) 332–338.
[48] J. Rajawat, N. Shukla, D.P. Mishra, Therapeutic targeting of poly(ADP-ribose) polymerase-1 (PARP1) in cancer: current developments, therapeutic strategies, and future opportunities, Med. Res. Rev. 37 (6) (2017) 1461–1491.
[49] A. Papa, D. Caruso, M. Strudel, S. Tomao, F. Tomao, Update on poly-ADP-ribose polymerase inhibition for ovarian cancer treatment, J. Transl. Med. 14 (2016) 267.
[50] D. Wang, M. Wang, N. Jiang, Y. Zhang, X. Bian, X. Wang, T.M. Roberts, J.J. Zhao, P. Liu, H. Cheng, Effective use of PI3K inhibitor BKM120 and PARP inhibitor Olaparib to treat PIK3CA mutant ovarian cancer, Oncotarget 7 (11) (2016) 13153–13166.